Local field effects at Li K edges in electron energy-loss spectra of Li, Li_2O and LiF

V. Mauchamp, P. Moreau,* G. Ouvrard, and F. Boucher
Institut des Matériaux Jean Rouxel, UMR 6502, Université de Nantes-CNRS, 2, Rue de la Houssinière, 44322 Nantes Cedex, France
(Received 2 July 2007; revised manuscript received 16 September 2007; published 14 January 2008)

Local field effects (LFEs) in low-losses of electron energy-loss spectra of Li, Li_2O, and LiF were calculated using the density functional theory under the generalized gradient approximation. By including the lithium 1*s* semicore state in the pseudopotentials, the amplitude of LFE was assessed all the way up to the Li K edge (from 0 to 80 eV). They are found to be much larger for semicore levels (2*s* of oxygen, 2*s* of fluorine, and 1*s* of lithium) than for the valence electron energy-loss region. LFEs at the Li K edge are studied in detail. In particular, for $q=0$ they are shown to increase with the inhomogeneities of the compounds (from Li to LiF). The influence of the magnitude and the direction of $\mathbf{q}$ is also presented. Both parameters have negligible effect in the case of Li metal but changes are quite substantial for Li_2O and LiF. This is in agreement with the isotropy and the delocalization of the metallic bonding as compared to the ionic one. LFEs at the Li K edge are, however, whatever the compound, much smaller than those observed at transition metal $M_{2,3}$ edges situated at similar energy positions. This result can be accounted for by considering the wave functions associated with the initial and final states involved in both edges. For lithium battery materials, most often presenting a transition metal edge close to the Li K edge, these findings imply significant consequences with respect to the interpretation of their electron energy-loss spectroscopy spectra. In particular, LFE can be expected to be stronger in positive electrodes than in negative ones.

DOI: 10.1103/PhysRevB.77.045117 PACS number(s): 79.20.Uv, 71.45.Gm, 78.20.Ci, 82.80.Pv

I. INTRODUCTION

Rechargeable lithium batteries are of considerable technological interest in the field of portable electronic devices.[1] They will soon be the standard electrical storage system in hybrid or all-electric vehicles. Much of the latest improvements in battery performance is based on innovative morphologies for the electrodes. Both the active material, through nanostructured particles or thin conducting coatings,[2–4] and the complete electrode, through the concept of composite electrodes,[5,6] have been optimized. As a consequence of these reduction in particle sizes and increase in the role of interfaces, transmission electron microscopy (TEM) has become an essential characterization technique.[7,8] In order to study compositions,[9] lithium insertion sites,[10] and charge compensation mechanisms occurring during battery utilization,[11] at a spatial resolution comparable with that of TEM, electron energy-loss spectroscopy (EELS) is an unrivaled analytical tool.[12] This probably explains why EELS is becoming increasingly popular in this area.[9–11,13–16] Most EELS studies focus on the host matrix of the electrode material and their transition metal, carbon or oxygen edges.[9,13–15] Very few concentrate on the sole common atom between all these batteries: the lithium atom.[10,11,16] We, however, showed recently that the electrochemical processes during lithium insertion in the electrode material could be investigated from a detailed analysis of the lithium K edge.[10] In order to accurately interpret the evolution of the experimental features, theoretical simulations were nevertheless shown to be indispensable.

Disregarding interference phenomena in the scattering process, which require special experimental settings to be observed,[17] a widely used approach to calculate the spectrum intensity at a given ionization edge (the doubly differentiated scattering cross section $d^2\sigma/d\Omega dE$) is the calculation of the dynamic form factor (DFF).[18] The expression of this quantity was derived long ago, within the first Born approximation,[19] in a single particle picture using the Bethe theory.[20] It has since been successfully applied to the simulation of K edges of various atoms in a wide range of materials.[21] Simulations of the low-loss part of an EELS spectrum (plasmons, excitations from valence or semicore states, etc.), however, require the inclusion of polarization effects (related to the real part of the dielectric function)[22] via the calculation of the loss function $\mathrm{Im}(-1/[\varepsilon_M(\mathbf{q},\omega)])$. These effects are usually not included in the DFF description. The entire macroscopic dielectric function of the material, $\varepsilon_M(\mathbf{q},\omega)=\varepsilon_{M,1}(\mathbf{q},\omega)+i\varepsilon_{M,2}(\mathbf{q},\omega)$, must, in fact, be calculated to obtain[12]

$$\mathrm{Im}\left(\frac{-1}{\varepsilon_M(\mathbf{q},\omega)}\right)=\frac{\varepsilon_{M,2}(\mathbf{q},\omega)}{\varepsilon_{M,1}(\mathbf{q},\omega)^2+\varepsilon_{M,2}(\mathbf{q},\omega)^2}. \quad (1)$$

In this expression, $\mathbf{q}$ and $E=\hbar\omega$ are the momentum and energy transferred from the fast electron to the material, respectively. The denominator explicitly reflects the screening effects induced by the polarization of the material on $\varepsilon_{M,2}(\mathbf{q},\omega)$,[23] $\varepsilon_{M,2}(\mathbf{q},\omega)$ being equivalent to the DFF for core edges. In the case of the Li K edge (situated around 55 eV), we recently showed that if a transition metal edge is present in its vicinity, these polarization effects should be taken into account. The simulation of the Li K edge consequently requires the calculation of the loss function, and not only that of $\varepsilon_{M,2}(\mathbf{q},\omega)$.[22]

Within the random phase approximation (RPA),[24] i.e., neglecting the exchange and correlation effects due to electron-hole interactions,[25] an important issue in the calculation of $\varepsilon_M(\mathbf{q},\omega)$, and thus of the loss function, is the inclusion of the crystal local field effects (LFEs) when passing from the microscopic dielectric function $\varepsilon(\mathbf{q},\omega)$ to the macroscopic scale.[26,27] The microscopic fields induced in the material by

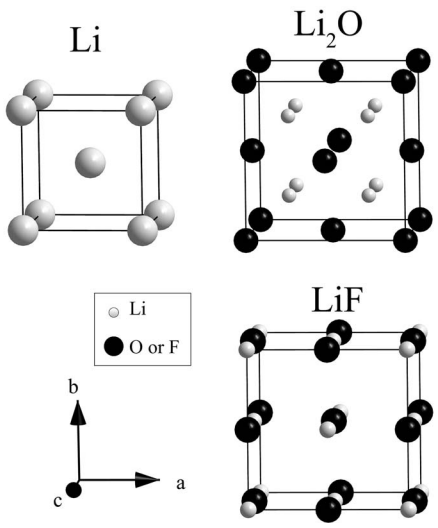

FIG. 1. Unit cells of Li, Li_2O, and LiF. These crystal structures can respectively be described in the following space groups: $Im\bar{3}m$, $Fm\bar{3}m$, and $Fm\bar{3}m$.

the exterior perturbation (the fast electron in an EELS experiment) and arising from the inhomogeneities of the electronic density of the material[28] were proven to have a dramatic effect on the calculation of the plasmons of semiconductors,[29] diamond,[30] or on the simulation of the excitations from semicore states such as the $N_{2,3}$ edges of Zr in ZrO_2,[31,32] of Sr in $SrTiO_3$,[33] or the $M_{2,3}$ edge of Ti in TiO_2.[34] In such cases, LFE reduce the calculated intensities thereby greatly improving the correlation between simulations and experiments. LFE can, however, be negligible in other cases, for example, in their effect on the plasmons of alkali metals such as Li or Na.[35,36] It is thus judicious to examine their magnitude at the Li K edge, which lies at energies comparable to those of the $N_{2,3}$ or $M_{2,3}$ edges of the previously mentioned transition metals. In order to acquire a broad knowledge of these effects at the Li K edge, we chose three model compounds: Li, Li_2O, and LiF. They host lithium atoms with different ionic characters (from metallic to very ionic) and present various electronic environments. These model compounds should thus cover the wide range of interactions present in lithium battery materials. The unit cells of these three compounds are represented in Fig. 1.

Beyond the fact that they are suitable model compounds with respect to the objective of this paper, simulations of Li K edges in these materials ought to be considered for their own worth. Li metal is widely studied due to its complex behavior under pressure,[37,38] even leading to superconductivity properties at low temperature.[39,40] Li_2O has practical interest for optical glasses, fast ionic conductors, or solid state batteries[41] and was even proposed as a potential blanket breeder material in nuclear reactors.[42] For many years, LiF has been and continues to be studied as a prototype for ionic bound insulators.[43–45]

A complete description of the dielectric function of wide gap insulators such as Li_2O and LiF clearly requires the inclusion of excitonic effects. Simulations of such effects at the Li K edge are well documented for Li_2O (Refs. 22 and 41) and LiF,[46,47] as well as for the low-loss spectrum of LiF.[45] Nevertheless, nothing has been reported about the magnitude of LFE at the Li K edge, as compared to those observed in low-loss spectra and, more importantly, with respect to the large LFE observed on transition metal edges. In view of a complete interpretation of lithium battery spectra, such a study is clearly necessary.

In this paper, we firstly present the conditions used to acquire the experimental spectra and then go on to detail the theoretical methods employed. We pay particular attention to the description of the inclusion of the lithium 1*s* semicore states in our pseudopotential. Li K edges with and without local field effects are then presented for $q=0$ and large q values in different crystallographic directions. The size of the LFE is then discussed with respect to these parameters for the three model compounds and with respect to those observed at the titanium $M_{2,3}$ edge.

II. EXPERIMENT

All samples were high-purity commercial products. The Li metal sample was prepared in a glovebox by cutting a thin slab from a lithium foil (99.9%, Alpha Aesar), after which it was placed directly into a Gatan 648 vacuum transfer sample holder and inserted into the microscope. In spite of all these precautions, most observed areas were slightly oxidized. However, as already mentioned by Liu *et al.*,[48] pure lithium crystals grow close to where the beam is focused and we collected our lithium spectra from these. The Li_2O powder was purchased from Alpha Aesar (99.5% purity). This sample was prepared under an inert argon atmosphere in a glovebox. Powders were crushed in hexane, deposited onto a holey carbon grid, and then inserted into the vacuum transfer sample holder. Prior to its introduction into the microscope, the sample holder containing the sample was placed under vacuum at 100 °C to remove surface contamination. Since the LiF powder (>99% purity, Alpha Aesar) is not moisture sensitive, the sample preparation was done in air, following the same procedure as for Li_2O. In this case though, the holey carbon grid was placed onto a cooling sample holder and spectra were recorded at liquid nitrogen temperature in order to minimize radiation damage.[49]

Experiments were performed with a TEM field emission gun Hitachi HF 2000 operated at 100 kV, and the spectra were recorded using a Gatan 666 parallel spectrometer. The energy resolution given by the zero loss peak (ZLP) full width at half maximum was 0.9 eV with a dispersion of 0.2 eV/channel. All spectra were dark count corrected. Convergence and acceptance angles were, respectively, 1.4 and 18.2 mrad. These angles imply an integration of the inelastic signal over a wide range of q. However, owing to the small characteristic angle for inelastic scattering at the Li K edge, most of the recorded intensity originates from very small q (below 0.2 $Å^{-1}$) and spectra should be compared to $\mathbf{q}=0$ calculations. In order to avoid irradiation damage, an uncondensed 400 nm diameter probe was used for Li and Li_2O. Total acquisition times were 2.5 and 0.25 s for the Li K edge (50–200 eV) and the low-loss region (0–150 eV), respectively. After acquisition, the spectra were first deconvoluted

using the ZLP with the PEELS program.[50] Multiple scattering was removed from the low-loss spectra following Stephen's procedure.[51]

III. THEORETICAL METHODS

The loss function is obtained from the macroscopic dielectric function [Eq. (1)]. For periodic systems, a quantity of this kind is related to the components of the microscopic dielectric matrix $\varepsilon_{\mathbf{GG}'}(\mathbf{q},\omega)$ [obtained by the Fourier transformation to reciprocal space of $\varepsilon(\mathbf{r},\mathbf{r}',\omega)$] by[26]

$$\varepsilon_M(\mathbf{q},\omega) = \frac{1}{[\varepsilon^{-1}_{\mathbf{GG}'}(\mathbf{q},\omega)]_{\mathbf{G}=\mathbf{G}'=0}}, \tag{2}$$

where $\mathbf{G}$ and $\mathbf{G}'$ are reciprocal lattice vectors. The LFE are thus related to the existence of the off-diagonal elements of $\varepsilon_{\mathbf{GG}'}(\mathbf{q},\omega)$. By neglecting them, the macroscopic dielectric function is reduced to the head of the microscopic dielectric matrix $\varepsilon_{00}(\mathbf{q},\omega)$.

It can be shown that, within the linear response theory, Eq. (2) is equivalent to[25]

$$\varepsilon_M(\mathbf{q},\omega) = 1 - \mathbf{v}_c(\mathbf{q})\chi(\mathbf{q},\omega), \tag{3}$$

where $\chi(\mathbf{q},\omega)$ is the response function of the system to the perturbation, also called polarizability, and $\mathbf{v}_c(\mathbf{q})$ the bare Coulomb interaction. $\chi(\mathbf{q},\omega)$ can be deduced from the polarizability of an hypothetical system of independent particles χ^0 by solving the following Dyson-like screening equation:[25]

$$\chi = \chi^0 + \chi^0(\bar{\mathbf{v}}_c + f_{\mathrm{xc}})\chi, \tag{4}$$

In our case, the exchange and correlation kernel f_{xc} is set to zero since we limit ourselves to the RPA level. The LFE are contained within the $\bar{\mathbf{v}}_c$ term, which is the microscopic part of the Coulomb interaction ($\mathbf{G} \neq 0$). The Fourier-transformed expression of χ^0 was derived in terms of independent transitions between the single particle states $|\psi\rangle$ of the considered system by Wiser[26] and, independently, by Adler,[27]

$$\chi^0_{\mathbf{GG}'}(\mathbf{q},\omega) = 2\sum_{i,f}(f_f - f_i)\frac{\langle\psi_i|e^{-i(\mathbf{q}+\mathbf{G})\cdot\mathbf{r}}|\psi_f\rangle\langle\psi_f|e^{i(\mathbf{q}+\mathbf{G}')\cdot\mathbf{r}}|\psi_i\rangle}{\omega - (\varepsilon_f - \varepsilon_i) + i\eta}, \tag{5}$$

where f_i and f_f are the occupation numbers and ε_i and ε_f the energies corresponding to the initial and final states with wave functions $|\psi_i\rangle$ and $|\psi_f\rangle$, respectively. In addition to $f_{\mathrm{xc}}=0$, by neglecting LFE (i.e., $\bar{\mathbf{v}}_c=0$), χ becomes equal to χ^0 which, once replaced in Eq. (3), gives the expression of the dielectric function of Ehrenreich and Cohen.[52]

Our calculations of the dielectric functions were performed using the DP code developed by Olevano *et al.*,[53] where the dielectric matrix is deduced from χ by the following relation:

$$\varepsilon^{-1}_{\mathbf{GG}'}(\mathbf{q},\omega) = \delta_{\mathbf{GG}'} + \mathbf{v}_c(\mathbf{q})_{\mathbf{G}}\chi_{\mathbf{GG}'}(\mathbf{q},\omega), \tag{6}$$

with

$$\chi_{\mathbf{GG}'} = (1 - \chi^0\bar{\mathbf{v}}_c)^{-1}_{\mathbf{GG}''}\chi^0_{\mathbf{G}''\mathbf{G}'}. \tag{7}$$

The single particle wave functions and energies entering Eq. (5) are Kohn-Sham orbitals and eigenvalues obtained from the plane wave pseudopotential code ABINIT.[54] Although rigorously not excitation energies,[55] the eigenvalues, as well as the eigenfunctions obtained with the density functional theory,[56] were proven to give very good results in such calculations.[31,34,57] Ground state calculations were performed within the generalized gradient approximation using the Perdew-Burke-Ernzerhof exchange and correlation potentials.[58] We used the Troullier-Martins norm-conserving pseudopotentials available in the ABINIT data base for oxygen and fluoride atoms.[59] The optimized pseudopotentials of Rappe *et al.*[60] were used for the lithium atom generated by the OPIUM code:[61] lithium 1*s* semicore states were included, thanks to the approach described by Rohlfing *et al.*[62] and the transferability of the pseudopotential was improved using the designed nonlocal pseudopotentials of Ramer and Rappe [63] A plane-wave cutoff of 108 Ry was necessary to achieve full convergence of the total energy for each compound. Ground state calculations were performed using $17\times17\times17$, $12\times12\times12$, and $13\times13\times13$ Monkhorst-Pack *k*-point meshes for Li, Li_2O, and LiF, respectively.[64] In order to achieve convergence on the calculation of the dielectric functions, 1000, 256, and 864 shifted *k*-points in the full Brillouin zone were, respectively, used for the calculation of $\chi^0_{\mathbf{GG}'}$. LFE were included by increasing the size of the polarizability matrix until spectra did not change. Convergence was reached with matrix sizes of 55×55, 59×59, and 65×65 for Li, Li_2O, and LiF, respectively; these values are very comparable to those reported in literature: 65×65 (Ref. 29) or 59×59 (Ref. 65) for the plasmon of Si or 57×57 (Ref. 33) for the $N_{2,3}$ edge of strontium, for example. Optimized unit cell parameters were used to perform the calculations of $\varepsilon_M(\mathbf{q},\omega)$. These agree well with the experimental ones: 3.433 Å for Li [expt.: 3.51 Å (Ref. 66)], 4.61 Å for Li_2O [expt.: 4.619 Å (Ref. 67)], and 4.057 Å for LiF [expt.: 4.03 Å (Ref. 68)].

In order to check on the quality of the pseudopotentials, we compared the loss functions calculated with DP without LFE to those obtained with the OPTIC program,[69] an extension of the WIEN2K code.[70,71] OPTIC generates the dielectric functions in the RPA, neglecting the LFE [i.e., $\varepsilon_{00}(0,\omega)$], using the all-electron Kohn-Sham orbitals and eigenvalues calculated with the WIEN2K code. The muffin tin radii used in WIEN2K for the Li atoms were 2.85, 1.70, and 1.91 bohr in Li metal, Li_2O, and LiF, respectively; for O and F, muffin tin radii were 1.88 and 1.91 bohr, respectively. Other calculation parameters are given in Table I. Comparisons between the OPTIC and DP loss functions are given in Figs. 2(a)–2(c) for Li, Li_2O, and LiF, respectively. The concordance between the all-electron (OPTIC) and the pseudopotential (DP) calculations is excellent. In the case of Li, the two spectra differ a little above 65 eV. This may be attributed to the fact that the inclusion of Li 1*s* semicore states requires the use of a Li^+ configuration as a reference for the generation of the pseudopotential, which is not optimum when dealing with covalent Li. The Li plasmon is also not reproduced in the DP calculation due to the fact that intraband transitions are not yet

TABLE I. Parameters used for the calculations of the ground state (GS) properties and the dielectric functions [$\varepsilon_M(\mathbf{q},\omega)$ or $\varepsilon_{0,0}(\mathbf{q},\omega)$]. k meshes from Monkhorst-Pack grids (Ref. 64). Unit cells taken from experimental data.

	ABINIT/DP				WIEN2K/OPTIC		
	GS		$\varepsilon_M(\mathbf{q},\omega)$		GS		$\varepsilon_{0,0}(\mathbf{q},\omega)$
	E_{cutoff} (Ry)	k mesh[a]	Shifted k-points[b]	Size of $\varepsilon_{\mathbf{G},\mathbf{G}'}(\mathbf{q},\omega)$	$R_{min}K_{max}$	k mesh[a]	k mesh[a]
Li	108	$17\times17\times17$	1000	55×55	7.0	$17\times17\times17$	$27\times27\times27$
Li_2O	108	$12\times12\times12$	256	59×59	7.0	$12\times12\times12$	$10\times10\times10$
LiF	108	$13\times13\times13$	864	65×65	7.0	$14\times14\times14$	$12\times12\times12$

[a]k mesh given with respect to the full Brillouin zone but only the irreducible part was used for the calculation.
[b]In the full Brillouin zone.

included in this program. Apart from these discrepancies on Li metal, the agreement between both methods demonstrates the quality of our pseudopotentials. From now on, all the calculations presented in this paper make use of the DP code.

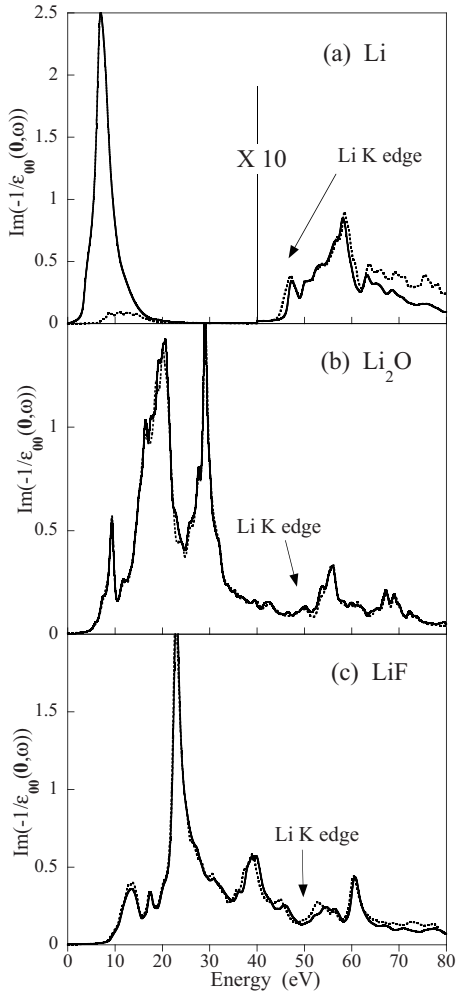

FIG. 2. Comparison between the loss functions obtained with OPTIC (full lines) and DP (dotted lines) for (a) Li, (b) Li_2O, and (c) LiF. Li K edge positions arrowed in each case. Calculations performed within the RPA for a vanishing momentum transfer and neglecting the LFE.

IV. RESULTS AND DISCUSSION

A. General comparison of low-loss spectra from 0 to 80 eV

The calculated low-loss spectra for Li, Li_2O, and LiF ($\mathbf{q}=0$, with or without LFE) are compared to those obtained experimentally in Figs. 3(a)–3(c). In all three compounds, we can identify the valence electron energy-loss spectrum (VEELS) region below 30, 25, and 35 eV in Li, Li_2O, and LiF, respectively. The VEELS intensity originates from all interband and intraband transitions between the valence and the conduction bands. The semicore states give rise to the higher energy peaks: the Li K edge around 55 eV ($1s$ level), the O L_1 edge around 28 eV ($2s$ level), and the F L_1 edge around 37 eV ($2s$ level).

In the case of Li metal, the vast discrepancy in the VEELS region resides in the noninclusion of intraband transitions. When compared with the OPTIC program calculation (including intraband contributions), the agreement with the experiment is very good in that region: the plasmon peak is observed at 7.0 eV with a shoulder at 4.2 eV to be compared with the calculated values: 7.3 and 3.5 eV, respectively. For Li_2O and LiF, the peaks appearing in the experiments are substantially reproduced (between 5 and 25 eV). However, a strong exciton is observed experimentally at 13.4 eV in the spectrum of LiF, which is not, as expected, obtained with our RPA calculation. The inclusion of an f_{xc} kernel [Eq. (4)] would be necessary in order to properly take the electron-hole interaction into account. This is, however, beyond the scope of this paper, in addition to the fact that other authors have already examined this feature in detail.[72,73] Small peaks below 10 eV can also be observed in the experiment. These structures, which are highly temperature dependent, have been widely studied in literature and can, in part, be attributed to electron traps formed by defects induced in the structure.[49]

The effects of local fields on the VEELS are somehow small, even when considering large peaks such as those at 18 eV in Li_2O and 22 eV in LiF. In the corresponding energy range, an examination of the real and imaginary parts of their dielectric functions shows that their shapes closely resemble

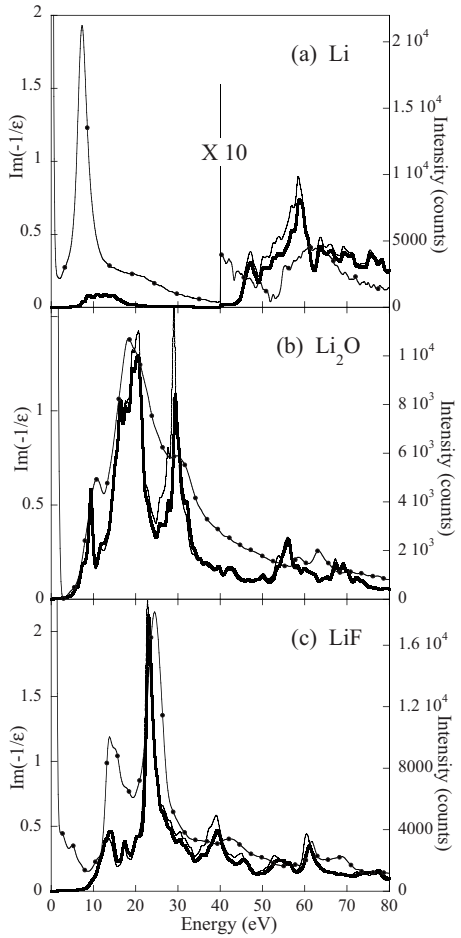

FIG. 3. Low-loss spectra in (a) Li, (b) Li_2O, and (c) LiF. Thin lines with black dots, experiments; thin lines, calculations without LFE; and thick lines, calculations with LFE.

those found for plasmon oscillations, as described by the Drude theory.[74] $\mathrm{Re}[\varepsilon_M(0,\omega)]$ crosses the energy axis and is a monotonous increasing function of the energy, while $\mathrm{Im}[\varepsilon_M(0,\omega)]$ is a monotonous decreasing one.[75] Not true plasmons, these peaks should rather be viewed as interband transitions exacerbated by a plasmonlike behavior.[76] Comparing the shape of these two structures, one can see that the interband plasmon of LiF is sharper than that observed for Li_2O. This is in agreement with the law stating that a plasmon full width at half maximum is proportional to the inverse of the derivative of $\mathrm{Re}[\varepsilon_M(0,\omega)]$ calculated at the plasma frequency.[35] These peaks are thus not the signature of transitions between localized states, but rather more like what is observed in the case of Drude metal plasmons, such as for Li or Na, which are not affected by the LFE for small momentum transfers.[35] This similarity explains the smallness of LFE on these peaks.

With regard to the semicore states, it should be noted that the absolute position of the Li K edges in the three compounds is not well reproduced when compared to experiments. This is a well documented problem that, from a formal point of view, excitation energies cannot be directly obtained from Kohn-Sham eigenvalues.[55] The calculated relative positions of these Li K edges, however, concur remarkably well with the experimental ones. Within a ±0.5 eV error bar, the values are 54, 57.1, and 60.1 eV (experiments) to be compared with 45.6, 48.7, and 51 eV (calculations). Even if the excitonic effects are not taken into account in our calculation, the influence of the ionicity of the Li atom is well reproduced. Energy shifts should consequently be meaningful when comparing various lithium compounds or different lithium sites in the same compound.

It is also quite remarkable that the LFE seem, in fact, to be larger for semicore states than for those found in the VEELS region. L_1 edges of oxygen (28 eV) and fluorine (37 eV) show significant local field effects. Some peak intensities can indeed be reduced by 30%. We will elaborate on the subject toward the end of this paper. For now, we shall focus on the main objective of this paper: the examination of local field effects at the Li K edge.

B. Local field effects at the Li K edge for q=0

Li K edges obtained with or without LFE and calculated with $\mathbf{q}=0$ are presented in Figs. 4(a)–4(c) (thick and thin lines, respectively) and compared to the corresponding experimental spectra (thin lines with dots). A constant Gaussian broadening of 0.4 eV was applied to each theoretical spectrum. As mentioned before, generalized gradient approximation (GGA) eigenvalues cannot be directly correlated to the real excitation energies of the system,[55] we thus shifted the theoretical energy scale in order to superimpose the calculated features to those observed experimentally (by approximately 8 eV for all three compounds).

The broad inspection of calculated spectra shows that they do not perfectly match the experimental ones. In particular, high energy peaks are calculated to be systematically more intense than those experimentally observed. In the case of Li, the 66 eV peak (energies are given with respect to the experimental energy scale at the top of Fig. 4) is too intense with respect to the 55 eV one. In the case of Li_2O, the 64 eV peak is too intense with respect to the 58 eV one and concerning LiF, the 69 eV peak is too intense with respect to the 62 eV one. This discrepancy is particularly strong in the case of Li_2O and LiF (insulators) and is related to the fact that electron-hole interactions are disregarded in our calculation. These "core hole effects" generate strong excitonic peaks at 58 and 62 eV on the experimental spectra relative to Li_2O (Ref. 41) and LiF,[44,77] respectively. Convolution of the theoretical spectrum with an energy-dependent Lorentzian function instead of a constant one,[78] in order to get a proper lifetime broadening, greatly improves the intensity ratios in the case of Li metal. Excitonic effects should nevertheless always be introduced in order to achieve a reasonable agreement [$f_{xc} \neq 0$ in Eq. (4)]. From these calculations, it can already be concluded that LFE, although small in some cases, have an effect on the Li K edge and that their extent can vary from one compound to another.

In order to better evaluate these effects, we present the quantity $(I_{\mathrm{LFE}}-I_{\mathrm{NLFE}})/I_{\mathrm{NLFE}}$ [Figs. 5(a)–5(c)]. In the energy range considered, for Li metal, Li_2O, and LiF, the relative variations are comprised between −27% and +8%, −30% and +15%, and −43% and +27%, respectively. LFEs are in

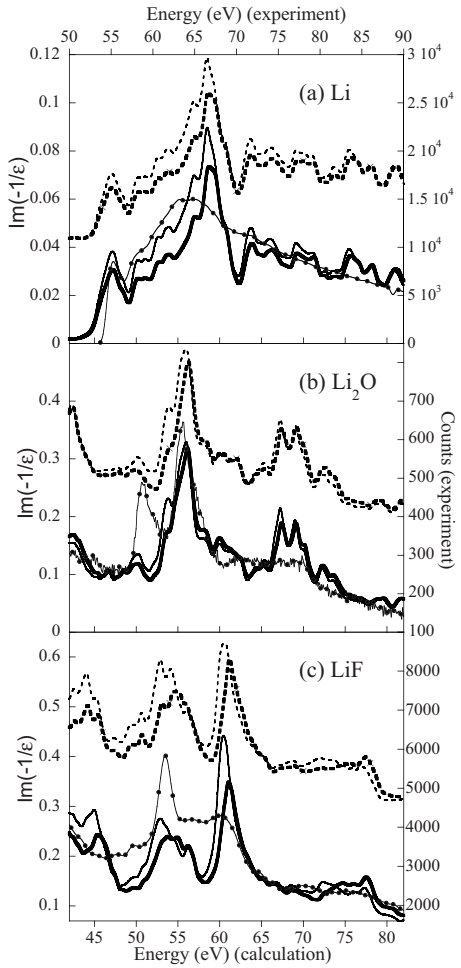

FIG. 4. Comparison between the Li K edges calculated without (thin lines) or with LFE (thick lines) for (a) Li, (b) Li_2O, and (c) LiF. Full lines, $\mathbf{q}=0$ and dashed lines, large q values. $q=0.67$ Å^{-1} in the [111] direction (Li), $q=0.62$ Å^{-1} in the [111] direction (Li_2O), and $q=0.82$ Å^{-1} in the [001] direction (LiF). All directions given in the conventional cell (Fig. 1). Large q spectra were shifted upward to facilitate visualization. Lines with black dots: experimental Li K edges for each compound. Experimental (top) and calculated (bottom) energy scales are different (8 eV shift).

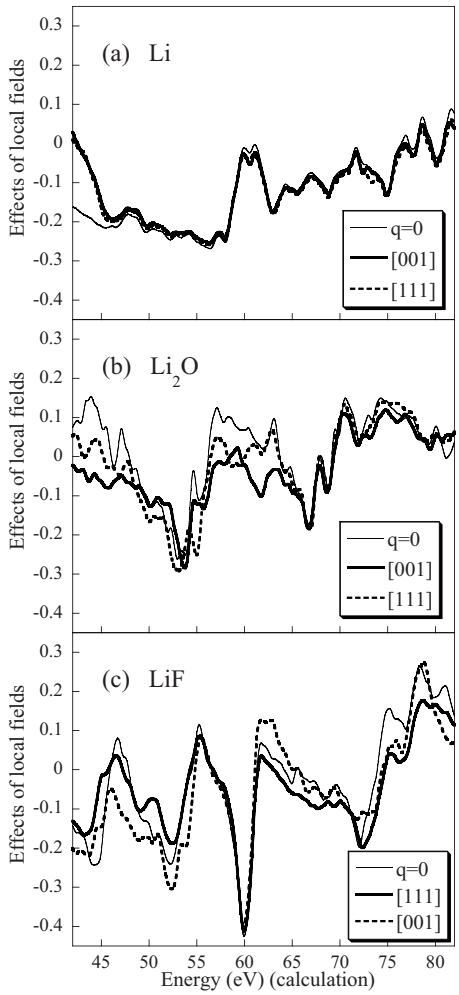

FIG. 5. Influence of the LFE, evaluated as $(I_{\mathrm{LFE}}-I_{\mathrm{NLFE}})/I_{\mathrm{NLFE}}$, at the Li K edge in (a) Li, (b) Li_2O, and (c) LiF. Thin lines: $\mathbf{q}=0$; thick lines: $q=0.58$ Å^{-1} in the [001] direction (Li), $q=0.72$ Å^{-1} in the [001] direction (Li_2O), and $q=0.71$ Å^{-1} in the [111] direction (LiF); dashed lines: $q=0.67$ Å^{-1} in the [111] direction (Li), $q=0.62$ Å^{-1} in the [111] direction (Li_2O), and $q=0.82$ Å^{-1} in the [001] direction (LiF). All directions given in the conventional cell (Fig. 1).

all compounds smaller than those observed at the Ti $M_{2,3}$ edge[34] (heights reduced by up to 60%) and at the Zr $N_{2,3}$ edge (up to 70% reduction),[31] which are situated at a similar energy position. As is generally reported in literature, we also find that LFEs tend to transfer the spectral weight to higher energies [for example, between 70 and 80 eV in Fig. 4(c)]. This trend appears even more clearly in Fig. 5(c) where the effect is negative over the 70–75 eV range, while found to be positive over the 75–80 eV range. The overall intensities of the lithium K edges follow the same tendency, with more negative values at the beginning of the spectrum (50–65 eV) than at its end (65 eV upward). If one were to integrate the total intensity from 50 to 100 eV, the intensity of the LFE spectra would, in fact, be close to that of the nonlocal field effect (NLFE) spectrum (within 10%). Despite the strong effects on narrow peaks at the beginning of the spectra, the actual scattering cross section at the lithium K edge is thus not greatly modified by the inclusion of LFE.

Finally, it clearly appears that the effects of the local fields increase from Li to Li_2O and LiF. For instance, the maxima of the relative intensity variations between I_{NLFE} and I_{LFE} rise from 27% to 30% and 43%, respectively, from Figs. 5(a)–5(c). This trend is coherent with an increase in the inhomogeneities in electron densities from Li to LiF.

C. Local field effects at the Li K edge for $\mathbf{q}\neq 0$

Larger values of q correspond to perturbations with shorter wave lengths and should consequently increase local field effects. We therefore performed calculations considering $\mathbf{q}\neq 0$ and present the results in Figs. 4(a)–4(c) (dashed-lines). The calculated spectra were shifted upward to facilitate their visualization. Convergence on the polarizability matrix size was checked again and was found to be unaf-

fected by the changes in the value of **q**. As anisotropic effects were reported in diamond[30] and predicted theoretically for cubic phases,[79] calculations were performed with momentum transfers along the main directions of the cubic lattice. As an example, we chose to present in Figs. 4(a)–4(c) the following spectra: $q=0.67$ Å^{-1} in the [111] direction for Li, $q=0.62$ Å^{-1} in the [111] direction for Li_2O, and $q=0.82$ Å^{-1} in the [001] direction for LiF. The direct inspection of the spectra with or without LFE does not allow a clear evaluation of the evolution of the LFE with the norm of q and as a function of the compound. We thus also calculated the $(I_{LFE}-I_{NLFE})/I_{NLFE}$ quantity and present the results in Figs. 5(a)–5(c) (dashed lines). For all compounds, LFE for these large q values (dashed lines) are not very different from those for $\mathbf{q}=0$ (thin lines). This is particularly clear in the case of Li metal and illustrates, once again, the rather homogeneous density in this metallic compound. As expected, the effects of local fields at the Li K edge in LiF (above 51 eV) are slightly enhanced for larger q values: relative variations present more negative values in the 51–55 eV range (dashed line compared to thin one) and more positive values in the 62–65 eV range.

The dashed lines in Figs. 5(a)–5(c) represent the LFE in the directions of the closest neighbors for the respective compounds (see Fig. 1). We also evaluated the LFE in other directions [thick lines in Figs. 5(a)–5(c)]. In the case of Li metal, LFEs are not sensitive to the chosen direction, in agreement with the nondirectionality of the metallic bonding. LFE clearly vary for different directions in the other two compounds. Their evolutions are, however, too complex to favor a simple explanation. The relative independence of the LFE on the directions, as compared to that found in diamond plasmon or in the Ti $M_{2,3}$ edge in TiO_2,[30,34] can be attributed to the marked spherical symmetry of the initial state (Li 1s).[34] Due to the enhanced anisotropy of the final states, one could, however, expect stronger dependence in noncubic compounds.

D. Discussion on the local field effect at the Li K edge

As previously stated, LFEs at the Li K edge are much smaller than those calculated for transition metals. This marked difference with excitations from semicore states of transition metals can be explained when considering the line of reasoning developed by Aryasetiawan *et al.*[80] on Ni and NiO. They showed that the strength of LFE at a given edge is related to the magnitude of a Coulomb integral for a charge density $\rho_\mu(\mathbf{r})-\bar{\rho}$, where $\rho_\mu(\mathbf{r})$ is the product of the two functions involved in the most important transition and $\bar{\rho}$ is the average of this product. We consequently present, in Figs. 6(a) and 6(b), the radial charge densities $D(r)=r^2R^2(r)$ for the Li 1s and Li 2p atomic wave functions and for the Ti 3p and Ti 3d atomic wave functions obtained from an all-electron atomic calculation (OPIUM program).[61] The comparison of the Li K edge (transition from the 1s to the 2p levels) with the Ti $M_{2,3}$ edge (transition from the 3p to the 3d levels) is particularly interesting since the LFE are quite large at the Ti $M_{2,3}$ edge.[34] Furthermore, Ti is representative of first row transition metals which are used in lithium batteries. It is

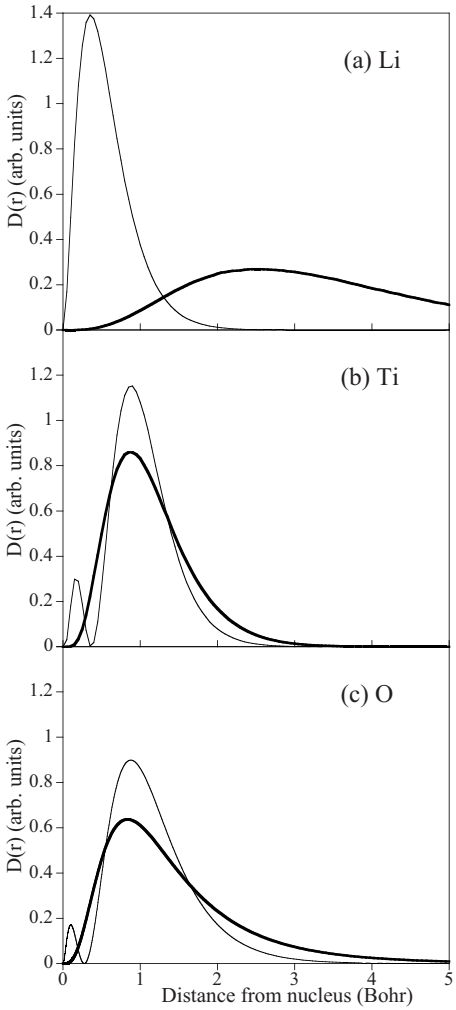

FIG. 6. Radial charge densities, $r^2R^2(r)$, for atomic wave functions of (a) Li, (b) Ti, and (c) O, obtained by an all electron calculation. (a) Thin line, Li 1s and thick line, Li 2p; (b) thin line, Ti 3p and thick line, Ti 3d; and (c) thin line, O 2s and thick line, O 2p.

evident from Fig. 6(b) that the radial charge densities of the Ti 3p and 3d wave functions have their maximum at the same distance from the nucleus. The interaction of both densities with each other (through the Coulomb interaction) is thus expected to be very large. LFEs are consequently important at the $M_{2,3}$ edge of this atom. In the case of the Li K edge, the situation is very different [Fig. 6(a)], with the maximum of 1s and 2p charge densities being far away from each other. LFEs at this edge are then expected to be rather small. In the context of lithium battery materials such as $LiFePO_4$,[9] LiV_3O_8,[81] $LiMO_2$ (M=Co, Ni, Mn),[11,14,15] all presenting a transition metal $M_{2,3}$ edge next to the Li K edge, LFEs are thus a complicated subject. The effects of local fields on EELS spectra are not a simple scaling factor on both lithium and transition metal edges. In most cases, the intensity variation of the transition metal edge, due to LFE, will modify the intensity observed on the lithium edge. Fitting methods for quantification of lithium may well be inappropriate. A detailed study of such a mutual influence between these edges is clearly necessary. The qualitative

argument developed by Aryasetiawan *et al.* shows the strong dependency of LFE on the localization—with respect to each other—of the initial and final electron wave functions involved in the transition. This interpretation, however, relies on an atomic description (charge densities for atoms) and puts aside solid state effects. Due to these effects, we showed that in the case of Li K edges, the strength of LFE can almost be doubled when going from Li metal to LiF [Figs. 5(a)–5(c)]. In the context of lithium battery compounds, this means that LFE can be expected to be stronger in positive electrodes (high potentials, marked ionic character) than in negative electrodes (low potentials, essentially elemental Li).[16] They may also vary as a function of the degree of charge or discharge of the battery since the lithium atom ionic character is not constant during the electrochemical process.[10] In order to obtain a precise and quantitative interpretation of lithium edges in lithium batteries, accurate simulations of the whole spectrum are then essential.

Finally, the situation for the O L_1 edge is somehow intermediate between the Li K edge and the Ti $M_{2,3}$ edge extreme cases, where the $2s$ and $2p$ radial charge distributions coincide significantly but are not as narrow as for Ti [Fig. 6(c)]. LFEs are thus expected to be strong, as observed in the calculation presented in Fig. 3(b), but still smaller than in the Ti case.

V. CONCLUSION

The influence of local field effects was investigated in this paper, both on the Li K edge and on the low-loss spectra of lithium based materials. In the case of Li, Li_2O, and LiF, LFEs are comparatively smaller in the VEELS region than for semicore levels. A detailed analysis of LFE, as a function of **q** and of the compounds, shows that they indeed increase as a function of inhomogeneities in electronic density and is also sensitive to the anisotropy of the materials. Aside from large excitonic effects, a comprehensive calculation of the Li K edge in very ionic compounds therefore requires the inclusion of LFE. They are, however, much smaller at the Li K edge compared, for example, to those observed at the $M_{2,3}$ edges of Ti or Zr. These findings substantiate the interpretation given by Aryasetiawan *et al.*,[80] stating that initial and final wave function charge densities should coincide significantly to produce large LFE. The marked LFE on O and F semicore levels can also be explained by following the same reasoning. The great variability of the LFE, as a function of the compound and the considered edges, implies that the understanding of lithium battery spectra is not straightforward. In particular, the influence of the strong transition metal edge LFE on the Li K edge will have to be studied and will be presented in the near future. A correction of the GGA eigenvalues will, however, have to be included since the absolute positions of the edges do not match the experimental ones. Even if calculations using the *GW* approximation would be ideal, a "scissors" operator might prove sufficient. A further improvement, also available in the DP code, is the inclusion of excitonic effects [through the f_{xc} term in Eq. (5)]. The influence of this interaction and the comparison of its effects on transition metal edges and the Li K edge should be very instructive and allow the precise quantification of lithium in most lithium battery materials.

ACKNOWLEDGMENTS

We would like to thank L. Reining, F. Sottile, and V. Olevano for having supplied us their DP code, for their help in its utilization, and for very fruitful discussions. The computations presented in this work were performed at the "Centre Régional de Calcul Intensif des Pays de la Loire" financed by the French Research Ministry, the "Région Pays de la Loire," and the University of Nantes.

*Philippe.Moreau@cnrs-imn.fr

[1] J. M. Tarascon and M. Armand, Nature (London) **414**, 359 (2001).
[2] A. Yamada, S. C. Chung, and K. Hinokuma, J. Electrochem. Soc. **148**, A224 (2001).
[3] C. Delacourt, P. Poizot, S. Levasseur, and C. Masquelier, Electrochem. Solid-State Lett. **9**, A352 (2006).
[4] M. Dubarry, J. Gaubicher, P. Moreau, and D. Guyomard, J. Electrochem. Soc. **153**, A295 (2006).
[5] D. Guy, B. Lestriez, and D. Guyomard, Adv. Mater. (Weinheim, Ger.) **16**, 553 (2004).
[6] D. Guy, B. Lestriez, R. Bouchet, and D. Guyomard, J. Electrochem. Soc. **153**, A679 (2006).
[7] A. Debart, L. Dupont, R. Patrice, and J.-M. Tarascon, Solid State Sci. **8**, 640 (2006).
[8] M. Dubarry, J. Gaubicher, P. Moreau, and D. Guyomard, J. Phys. Chem. Solids **67**, 1312 (2006).
[9] L. Laffont, C. Delacourt, P. Gibot, M. Y. Wu, P. Kooyman, C. Masquelier, and J. M. Tarascon, Chem. Mater. **18**, 5520 (2006).
[10] V. Mauchamp, P. Moreau, L. Monconduit, M.-L. Doublet, F. Boucher, and G. Ouvrard, J. Phys. Chem. C **111**, 3996 (2007).
[11] J. Graetz, C. C. Ahn, R. Yazami, and B. Fultz, J. Phys. Chem. B **107**, 2887 (2003).
[12] R. F. Egerton, *Electron Energy-Loss Spectroscopy in the Electron Microscope* (Plenum, New York, 1996).
[13] P. Diaz-Carrasco, P. Moreau, D. Guyomard, A. Kuhn, and F. Garcia-Alvarado, J. Phys. Chem. Solids **67**, 1295 (2006).
[14] J. Graetz, A. Hightower, C. C. Ahn, R. Yazami, P. Rez, and B. Fultz, J. Phys. Chem. B **106**, 1286 (2002).
[15] S. Miao, M. Kocher, P. Rez, B. Fultz, Y. Ozawa, R. Yazami, and C. C. Ahn, J. Phys. Chem. B **109**, 23473 (2005).
[16] A. Hightower, C. C. Ahn, and B. Fultz, Appl. Phys. Lett. **77**, 238 (2000).
[17] P. Schattschneider, M. Nelhiebel, H. Souchay, and B. Jouffrey, Micron **31**, 333 (2000).
[18] K. Sturm, Z. Naturforsch., A: Phys. Sci. **48**, 233 (1993).
[19] B. L. Moiseiwitsch and S. J. Smith, Rev. Mod. Phys. **40**, 238 (1968).
[20] M. Inokuti, Rev. Mod. Phys. **43**, 297 (1971).
[21] C. Hebert, Micron **38**, 12 (2007).

[22] V. Mauchamp, F. Boucher, G. Ouvrard, and P. Moreau, Phys. Rev. B **74**, 115106 (2006).
[23] P. Schattschneider, Ultramicroscopy **28**, 1 (1989).
[24] P. Nozières and D. Pines, Phys. Rev. **109**, 741 (1958).
[25] G. Onida, L. Reining, and A. Rubio, Rev. Mod. Phys. **74**, 601 (2002).
[26] N. Wiser, Phys. Rev. **129**, 62 (1963).
[27] S. L. Adler, Phys. Rev. **126**, 413 (1962).
[28] W. Hanke, Adv. Phys. **27**, 287 (1978).
[29] B. Arnaud and M. Alouani, Phys. Rev. B **63**, 085208 (2001).
[30] S. Waidmann, M. Knupfer, B. Arnold, J. Fink, A. Fleszar, and W. Hanke, Phys. Rev. B **61**, 10149 (2000).
[31] L. K. Dash, N. Vast, P. Baranek, M.-C. Cheynet, and L. Reining, Phys. Rev. B **70**, 245116 (2004).
[32] L. K. Dash, F. Bruneval, V. Trinité, N. Vast, and L. Reining, Comput. Mater. Sci. **38**, 482 (2006).
[33] E. E. Krasovskii and W. Schattke, Phys. Rev. B **60**, R16251 (1999).
[34] N. Vast, L. Reining, V. Olevano, P. Schattschneider, and B. Jouffrey, Phys. Rev. Lett. **88**, 037601 (2002).
[35] K. Sturm, Adv. Phys. **31**, 1 (1982).
[36] Y.-G. Jin and K. J. Chang, Phys. Rev. B **59**, 14841 (1999).
[37] J. B. Neaton and N. W. Ashcroft, Nature (London) **400**, 141 (1999).
[38] R. E. Alonso, S. Sharma, C. Ambrosch-Draxl, C. O. Rodriguez, and N. E. Christensen, Phys. Rev. B **73**, 064101 (2006).
[39] K. Shimizu, H. Ishikawa, D. Takao, T. Yagi, and K. Amaya, Nature (London) **419**, 597 (2002).
[40] V. V. Struzhkin, M. I. Eremets, W. Gan, H.-K. Mao, and R. J. Hemley, Science **298**, 1213 (2002).
[41] N. Jiang and J. C. H. Spence, Phys. Rev. B **69**, 115112 (2004).
[42] C. E. Johnson, K. R. Kummerer, and E. Roth, J. Nucl. Mater. **155-157**, 188 (1988).
[43] J. R. Fields, P. C. Gibbons, and E. Schnatterly, Phys. Rev. Lett. **38**, 430 (1977).
[44] J. P. Stott, S. L. Hulbert, F. C. Brown, B. Bunker, T. C. Chiang, T. Miller, and K. H. Tan, Phys. Rev. B **30**, 2163 (1984).
[45] W. A. Caliebe, J. A. Soininen, E. L. Shirley, C.-C. Kao, and K. Hämäläinen, Phys. Rev. Lett. **84**, 3907 (2000).
[46] R. Brydson, J. Bruley, and J. M. Thomas, Chem. Phys. Lett. **149**, 343 (1988).
[47] E. L. Shirley, J. Electron Spectrosc. Relat. Phenom. **137-140**, 579 (2004).
[48] D.-R. Liu, G. Rommal, and D. B. Williams, J. Electron Microsc. Tech. **4**, 381 (1985).
[49] F. Golek and W. J. Sobolewski, Solid State Commun. **110**, 143 (1999).
[50] P. Fallon and C. A. Walsh, *PEELS Program*, (University of Cambridge, England, 1996).
[51] A. P. Stephen, Ph.D. thesis, University of Cambridge, 1980.
[52] H. Ehrenreich and M. H. Cohen, Phys. Rev. **115**, 786 (1959).
[53] V. Olevano, L. Reining, and F. Sottile, http://theory.lsi.polytechnique.fr/codes/dp/dp.html, 1998.
[54] X. Gonze, J.-C. Beuken, R. Caracas, F. Detraux, M. Fuchs, G.-M. Rignanese, L. Sindic, M. Verstraete, G. Zerah, F. Jollet, M. Torrent, A. Roy, M. Mikami, P. Ghosez, J.-Y. Raty, and D. C. Allan, Comput. Mater. Sci. **25**, 478 (2002).
[55] R. O. Jones and O. Gunnarsson, Rev. Mod. Phys. **61**, 689 (1989).
[56] R. G. Parr and W. Yang, *Density-Functional Theory of Atoms and Molecules* (Oxford Science, Oxford, 1989).
[57] V. J. Keast, J. Electron Spectrosc. Relat. Phenom. **143**, 99 (2005).
[58] J. P. Perdew, K. Burke, and M. Ernzerhof, Phys. Rev. Lett. **77**, 3865 (1996).
[59] N. Troullier and J. L. Martins, Phys. Rev. B **43**, 1993 (1991).
[60] A. M. Rappe, K. M. Rabe, E. Kaxiras, and J. D. Joannopoulos, Phys. Rev. B **41**, 1227 (1990).
[61] OPIUM (http://opium.sourceforge.net).
[62] M. Rohlfing, P. Krûger, and J. Pollmann, Phys. Rev. B **57**, 6485 (1998).
[63] N. J. Ramer and A. M. Rappe, Phys. Rev. B **59**, 12471 (1999).
[64] H. J. Monkhorst and J. D. Pack, Phys. Rev. B **13**, 5188 (1976).
[65] S. G. Louie, J. R. Chelikowsky, and M. H. Cohen, Phys. Rev. Lett. **34**, 155 (1975).
[66] M. R. Nadler and C. P. Kempter, Anal. Chem. **31**, 2109 (1959).
[67] E. Zintl, A. Harder, and B. Dauth, Z. Elektrochem. **40**, 588 (1934).
[68] P. Cortona, Phys. Rev. B **46**, 2008 (1992).
[69] C. Ambrosch-Draxl and J. O. Sofo, J. Phys.: Condens. Matter **175**, 1 (2006).
[70] P. Blaha, K. Schwarz, G. K. H. Madsen, D. Kvaniscka, and J. Luitz, WIEN2K, an augmented plane wave+local orbitals program for calculating crystal properties Technische Universität Wien, Austria, 2001.
[71] P. Blaha, K. Schwarz, G. K. H. Madsen, D. Kvaniscka, and J. Luitz, WIEN2K User's guide, 2001 (http://www.wien2k.at/reg_user/textbooks).
[72] M. Rohlfing and S. G. Louie, Phys. Rev. Lett. **81**, 2312 (1998).
[73] J. A. Soininen and E. L. Shirley, Phys. Rev. B **61**, 16423 (2000).
[74] R. E. Hummel, *Electronic Properties of Materials; An Introduction for Engineers* (Spinger-Verlag, Berlin, 2000).
[75] V. Mauchamp, Ph.D. thesis, University of Nantes, 2006.
[76] R. E. Dietz, M. Campagna, J. N. Chazalviel, and H. R. Shanks, Phys. Rev. B **17**, 3790 (1978).
[77] J. A. Soininen and E. L. Shirley, Phys. Rev. B **64**, 165112 (2001).
[78] P. Moreau, F. Boucher, G. Goglio, D. Foy, V. Mauchamp, and G. Ouvrard, Phys. Rev. B **73**, 195111 (2006).
[79] S. R. Nagel and T. A. Witten, Jr., Phys. Rev. B **11**, 1623 (1975).
[80] F. Aryasetiawan, O. Gunnarsson, M. Knupfer, and J. Fink, Phys. Rev. B **50**, 7311 (1994).
[81] F. Boucher, N. Bourgeon, K. Delbe, P. Moreau, D. Guyomard, and G. Ouvrard, J. Phys. Chem. Solids **67**, 1238 (2006).